Index Modulation for OFDM RadCom Systems

Index Modulation for OFDM RadCom Systems

Gaojian Huang [1,2], Yuan Ding [3] ✉, Shan Ouyang [1,4], Vincent Fusco [2]
[1] School of Information and Communications, Guilin University of Electronic Technology, Guilin 541004, China
[2] Institute of Electronics, Communications and Information Technology (ECIT), Queen's University of Belfast, Belfast BT3 9DT, UK
[3] The Institute of Sensors, Signals and Systems (ISSS), Heriot-Watt University, Edinburgh EH14 4AS, UK
[4] State and Local Joint Engineering Research Centre for Satellite Navigation and Location Service (Guilin University of Electronic Technology), Guilin, Guangxi, China
✉ *E-mile: yuan.ding@hw.ac.uk*

Abstract: In this paper, a novel Radar and wireless communication fusion system, namely RadCom, using orthogonal frequency division multiplexing index modulation (OFDM-IM) waveforms is studied. From the communication perspective, information is conveyed not only through modulated OFDM subcarriers but also by the active subcarrier indices that are dynamically updated at the transmitted symbol rates. When compared with conventional OFDM communication systems, only a subset of subcarriers is activated in the proposed OFDM-IM system, which reduces signal peak-to-average-ratios (PAPRs), leading to enhanced power amplifier (PA) efficiency. From the Radar sensing perspective, the Radar range-velocity profile obtained using compressed sensing (CS) approach is simulated and presented. It is shown that OFDM-IM RadCom system can enhance the transmission data rates when low-order modulation schemes are adopted, e.g. binary phase shift keying (BPSK), and maintain similar Radar performance compared with the OFDM counterpart when the system is carefully designed.

1 Introduction

The Radar and wireless communication fusion system refers to a system that provides Radar and communication functions using a single waveform. In other words, using a joint waveform to achieve both Radar and wireless communication functions. The integration of Radar sensing and wireless communications is of great interest [1]–[3], because of the scarcity of the spectrum resources and the requirements for multi-functional applications, such as autonomous vehicles where sensing the surrounding environment and communications among vehicles and/or infrastructures are critical to the traffic efficiency and road safety. In these integrated systems, Radar sensing and wireless data transfer operate concurrently through appropriate design of signal waveforms. Meanwhile, the two functions could also assist each other. For example, the communication module could use Radar sensing to track legitimate users for authentication purpose and improving communication link budget. While with the help of the wireless data exchange, cooperative distributed Radar sensor networks can be constructed. The resulting fusion systems are commonly termed 'RadCom' [1]. As an application example, the 'self-driving' lorries will be tried out on major British roads, in which two vehicle platoons are required to maintain communication links and sense their surroundings using Radar technologies [4].

In recent years orthogonal frequency division multiplexing (OFDM) waveforms have been adopted for this purpose [1], [5]. The single carrier RadCom system, i.e., a RadCom system whose transmitter only radiates a single carrier waveform that are usually modulated to obtain a quasi-optimum autocorrelation property which can guarantee a dynamic range of the measurement when applying to Radar, was also introduced [1]. In [3], linear frequency modulated (LFM) pulses, i.e. chirp signals, were designed, not only for Radar sensing, but also conveying data. However, the transmitted symbol rate is determined by the chirp rate, resulting in a poor spectral efficiency. Compared with these RadCom systems, OFDM can improve the range and Doppler resolutions, from the Radar perspective, meanwhile it also improves transmission data rates, from the communication perspective. However, it is well-known that the high peak-to-average power ratio (PAPR) of the OFDM signals requires the power amplifier (PA) to operate at high back-off points, thus, significantly reducing the PA and the whole system efficiency. To address this issue, some works have been conducted, such as using amplitude clipping, coding schemes, Partial Transmission Sequence (PTS) and Selective Mapping (SLM) techniques [6]. The amplitude clipping technique employs clipping the peak envelope of the input signal to reduce the PAPR, which is a simplest technique compared with other PAPR reduction techniques. However, it leads to both in-band and out-of-band interferences, destroying the orthogonality among the subcarriers. While the coding technique is to select those codewords that minimise or reduce the PAPR. Compared with the clipping, the problem of distortion and out-of-band radiation does not exist in coding. This coding technique, however, suffers from high complexity. Meanwhile, the PTS and SLM techniques also have the problem of high complexity. In addition, Tone Reservation (TR) and Tone Injection (TI) techniques were proposed to reduce the PAPR in [7]. These two efficient techniques are based on adding a data-block-dependent time domain signal to the original multicarrier signal to reduce the PAPR. Compared with TR technique, The TI technique is more problematic since the injected signal occupies the frequency band as the information bearing signals.

Recently, a variant OFDM waveform, named OFDM-index modulation (OFDM-IM), has been presented [8]. Index modulation (IM) is a novel transmission technique that is capable of achieving high spectral efficiency by way of creating an additional dimension in the subcarrier domain

compared with the conventional modulation techniques. More specifically, in the OFDM-IM, only a subset of subcarriers is activated to carry constellation symbols, meanwhile, the active subcarrier indices are also designed to convey additional binary information. Thus, information is transmitted not only through modulated radio frequency (RF) carriers but also by the indices of dynamically activated OFDM subcarriers. Later the OFDM-IM has been intensively investigated under the communication context [9]–[11]. In [9], A thorough study of OFDM-IM scheme was presented and compared with the frequency and quadrature amplitude modulation (FQAM) and the classic OFDM schemes, showing the superiority of the OFDM-IM scheme in spectral efficiency and signal-to-noise ratio (SNR) gains. The OFDM-IM concept was further extended to multiple-input multiple-output (MIMO) scenarios in [10]. In [11], the achievable rate of OFDM-IM with channel state information at the receiver was studied and the lower bound was derived in a closed-form, indicating that the optimal subcarrier activation strategy which maximises the superiority of OFDM-IM over classical OFDM can be predicted. Apart from the benefits of low transceiver complexity and flexibly adaptable spectral efficiency, the OFDM-IM enjoys reduced PAPR [12].

This paper is dedicated to introducing OFDM-IM waveforms for RadCom systems by investigating the following aspects:

- For the Radar sensing functionality, the ambiguity functions of the conventional OFDM and the proposed OFDM-IM RadCom waveforms are firstly computed to compare their resolutions and peak-to-side-lobe ratios (PSLs) in both range and Doppler frequency domains. Then, we focus on using the compressed sensing (CS) method to obtain the Radar range-velocity profile in the proposed OFDM-IM RadCom system;
- For wireless data transfer purpose, data rates and associated bit error rates (BERs) are studied.

The remainder of this paper is organized as follows: In Section 2, the RadCom system model and its operational principle are presented. Sections 3 and 4 are dedicated to its performance assessment, with regard to Radar sensing and the PA efficiency in Section 3, leaving spectral efficiency and the BER in Section 4. Finally, Section 5 concludes the paper.

2 Proposed OFDM-IM RadCom system

In this section, we first describe OFDM RadCom, then the proposed OFDM-IM RadCom is introduced and elaborated along with its design details. Throughout what follows the transmitted baseband signal waveform is denoted as $x(t)$, $y_1(t)$ is the received waveform at the far-field target, and $y_2(t)$ is the detected backscattering signals from the target for Radar processing. To better demonstrate the RadCom systems, a typical vehicular RadCom scenario is illustrated in Fig. 1. The RadCom waveform radiated from the transmit (Tx) car conveys information data to other 'targets', e.g. other cars. Meanwhile, the Tx car detects the backscattered signals from other cars to perform Radar processing, identifying the targets' range and velocity. Therefore, in a RadCom system, for the communication link, the receiver is located in the far-field. While for the Radar link, the receiver is co-located with the

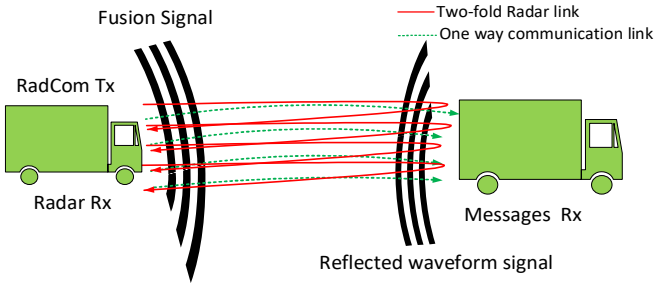

Fig. 1 *An example vehicle-to-vehicle (V2V) RadCom application scenario.*

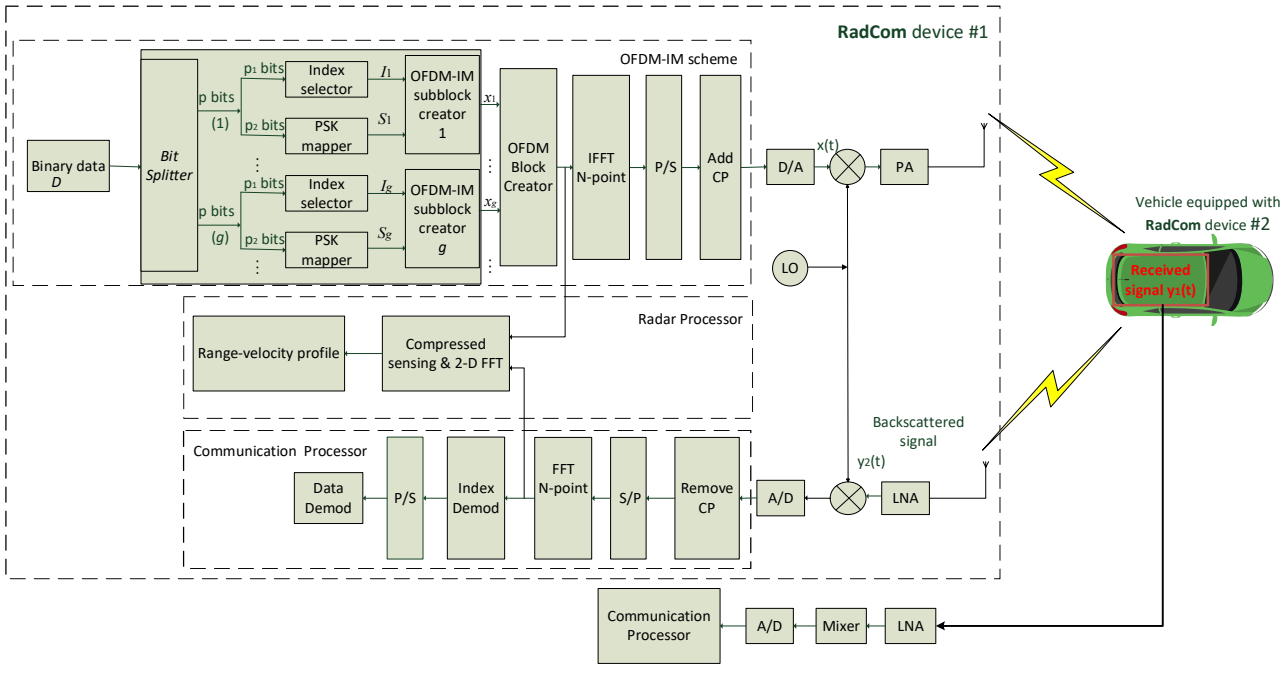

Fig. 2 *Block diagram of the proposed OFDM-IM RadCom system architecture.*

transmitter, meaning that the propagation channels are bi-directional.

2.1. OFDM RadCom model

The OFDM waveform is popular for wireless communication systems because it can better combat frequency selective channel fading as compared with the single-carrier waveform. It also offers higher transmission data rates as data can be modulated in parallel onto multiple orthogonal subcarriers. Therefore, OFDM has been adopted in many modern wireless communication systems, such as IEEE 802.11a/g, IEEE 802.16, and 4G Long Term Evolution (LTE) [13]. In the Radar community Levanon first proposed a multi-frequency complementary phase coded (MCPC) signal that could achieve low side-lobes and ambiguities in the range domain [14]. This approach shares a similar concept with later OFDM Radar research [15].

Exploiting OFDM waveforms for joint Radar and communication, i.e. OFDM RadCom, has been previously discussed in e.g. [1], [2], [5]. Compared with single-carrier, multicarrier OFDM waveforms, enjoy greater frequency bandwidth, and are able to enhance RadCom system performance. In particular, they can improve range resolution and dynamic range for target detection, while on the other hand, support higher data rates.

An OFDM baseband signal $x(t)$ can be expressed as

$$x(t) = \sum_{\mu=0}^{N_{\text{sym}}-1} \sum_{\eta=0}^{N-1} a_{(\mu,\eta)} \exp\left(j2\pi f_\eta t\right) \text{rect}\left(\frac{t-\mu T}{T}\right). \quad (1)$$

The function 'rect[$(t-\mu T)/T$]' represents a time-domain rectangular window of duration T. μ denotes the OFDM symbol index with the total number of N_{sym}. η represents the OFDM subcarrier index, from 0 to $N-1$. Complex-valued $a_{(\mu,\eta)}$ is modulated upon the η^{th} subcarrier in the μ^{th} OFDM symbol. This subcarrier has a baseband frequency f_η. When the condition $f_\eta = \eta/T$ is satisfied, the subcarriers are orthogonal in frequency domain.

In the OFDM RadCom system, $x(t)$, modulated by RF carrier, is radiated, and then received by a far-field target as $y_1(t)$. As the Rx receiver co-located with the Radar Tx, the range and velocity of the targets can be recovered from the backscattered $y_2(t)$ via the Radar signal processor, see Fig. 2. It is noted for the two RadCom devices, shown in Fig. 2, when the RadCom device #1 served as Radar target, the vehicle RadCom device #2 would act as transmitter, and vice versa. Thus the RadCom device #2 also has the capability of both transmit and receive communication signals to/from the RadCom device #1. On the other hand, the interference cancellation between signals received for Radar and communications is required in order to obtain higher signal-to-noise plus interference ratio. This can be achieved by exploiting the conventional OFDM demodulation techniques including steps such as time and frequency synchronisation, residue time and fine frequency estimation, and signal reconstruction and cancellation, as described in [16].

2.2. OFDM-IM RadCom system

OFDM-IM provides a novel means of conveying information by dynamically mapping the data bits to the active subcarrier indices. Compared with conventional OFDM, only a subset of subcarriers is activated in the OFDM-IM scheme, while others are suppressed. To perform OFDM-IM, the information bit stream D, to be conveyed to the far-field target, is first divided into G groups, each is then further separated into two parts p_1 and p_2 [8]. Each of the G groups, referred to an OFDM-IM sub-block hereafter, is assigned the same number of subcarriers. It is assumed that $p_1 + p_2 = p$ is the same for each group, thus $Gp = D$. The first p_1 bits of the incoming p-bit stream determine the active subcarrier indices assigned to the subcarriers allocated to its group, and the remaining p_2 bits are associated with the conventional digital modulated RF data information carriers transferred through the active subcarriers. Each OFDM-IM sub-block operates independently.

The transmitter architecture of the OFDM-IM for the RadCom system is the same as that used in the OFDM-IM communication system. The only difference exists at the receiver end, see Fig. 2. Apart from the wireless data transfer to the receiver, Radar signal processing is also required at the OFDM-IM transceiver node post the backscattered signals from the far-field targets being detected.

To facilitate the discussion, the transmitter settings are now presented; Assume there are N available OFDM subcarriers, which is also the order of the inverse fast Fourier transform (IFFT) module. G is the total number of the groups. In each OFDM-IM sub-block, and for each transmitted symbol, k out of n ($n = N/G$) subcarriers are selected, which is determined by the baseband data of p_1 bits in that bits group. The remaining p_2 bits in the same bits group go through standard IQ modulators before being mapped onto the selected active subcarriers. $K = kG$ is the total number of active subcarriers.

In the g^{th} OFDM-IM sub-block ($g = 1, 2, \ldots, G$), we use I_g to represent the selected subcarrier indices,

$$I_g = \{i_{g,1}, \ldots, i_{g,k}\}, \quad (2)$$

where $i_{g,\gamma} \in \{0, 1, \ldots, n-1\}$, $\gamma = 1, 2, \ldots, k$, and $i_{g,a} \neq i_{g,b}$ when $a \neq b$. As we discussed earlier, I_g is determined by the baseband data p_1 bits, indicating

$$p_1 = \lfloor \log_2(C(n,k)) \rfloor, \quad (3)$$

where $C(n, k)$ refers to the number of k-combinations out of a set of n elements. Generally, $k \leq n$. In order to simplify formulation later, specifically, we define $C(\gamma - 1, \gamma) = 0$. Operator '$\lfloor . \rfloor$' denotes integer floor function.

The baseband data of p_2 bits are associated with M-ary IQ modulations applied upon the selected k subcarriers. Thus,

$$p_2 = k \cdot \log_2 M. \quad (4)$$

The mapping procedures in each sub-block, from baseband bits p_1 to k subcarrier indices, are now presented as below [8];

- The p_1 bits are first converted to a decimal number c, using

$$c = \sum_{m=0}^{p_1-1} 2^m \, p_1^{(m)}, \quad (5)$$

where $p_1^{(m)}$ denotes the m^{th} bit in the p_1 bit sequence. Here $0 \le c \le C(n, k) - 1$;

- Map the decimal number c to a strictly decreasing sequence $\{j_k, j_{k-1}, \ldots, j_1\}, j_\gamma \in \{0, 1, 2, \ldots, n-1\}$, and $j_a \ne j_b$ when $a \ne b$; j_k is the largest natural number satisfying $C(j_k, k) \le c$. In case when $c = 0$, we assign j_k with $k - 1$. Then, j_{k-l} is the natural number satisfying

$$C(j_{k-l}, k-l) \le c - \sum_{l=1}^{k-1} C(j_{k-l+1}, k-l+1) \le C(j_{k-l}+1, k-l) \cdot \tag{6}$$

- The sequence $\{j_k, j_{k-1}, \ldots, j_1\}$, termed as J hereafter, contains the selected active subcarrier indices in that bit group.

The above mapping procedures offers a one-to-one mapping between the p_1 bit sequences and the selected subcarrier indices J, so that the original transmitted bits can be uniquely recovered through the detected subcarrier indices at the receiver side. To facilitate understanding, as an example, when $n = 16$ and $k = 4$, it is calculated using (3) that $p_1 = \lfloor \log_2(C(16, 4)) \rfloor = 10$. We assume that the p_1 bit sequence is '1100001011'. Using (5), we get the corresponding decimal number $c = 779$. Then, as $C(13, 4) = 715 < c = 779 < C(14, 4) = 1001$, 13 is the largest number that satisfies the combinational number smaller than c, i.e. $j_4 = 13$. Similarly, via (6) j_3, j_2, and j_1 can be calculated, i.e. 8, 4, and 2, respectively. Therefore, the sequence J of {13, 8, 4, 2} contains the selected subcarrier indices, which is mapped from the information bits '1100001011' by the 'Index Selector' module in that bits group. Some other mapping examples are listed in Table 1.

It is noted that the number of possible subcarrier index combinations $C(n, k)$ is always greater than the required number for p_1 bit representation. For the example used in Table 1, $C(16, 4) = 1820 > 2^{p_1} = 1024$. This indicates some subcarrier combinations, i.e. 1820 – 1024 = 796, will not be used. Obviously, those unused combinations need to be pre-excluded at the receiver side in order to reduce the probability of incorrectly recovering the active subcarrier indices through the received noise-contaminated OFDM-IM signals. For this purpose, an algorithm is developed and will be presented in Section 4.

Table 1 The mapping relationship between bit sequences p_1 of 10-bit and active subcarrier indices J.

p_1 (10 bits)	Decimal c	Subcarrier index sequence J
0000000000	0	3, 2, 1, 0
0000000001	1	4, 2, 1, 0
…	…	…
100001011	779	13, 8, 4, 2
…	…	…
1111111110	1022	14, 6, 2, 0
1111111111	1023	14, 6, 2, 1

Table 2 Example OFDM-IM system with $N = 64$. k and K are one-to-one mapped.

G	n	k	K
32	2	1	32
16	4	1, 2, 3	16, 32, 48
8	8	1, 2, 3, 4, 5, 6, 7	8,16, 24, 32, 40, 48, 56
4	16	1, 2, 3, 4, 5, 6, 7, 8, 9, 10, 11, 12, 13, 14, 15	4, 8, 12, 16, 20, 24, 28, 32, 36, 40, 44, 48, 52, 56, 60

In the transmitter module of the proposed OFDM-IM RadCom system, we use I_g and S_g to represent the sequence of the active subcarrier indices and the vector of M-ary data symbols assigned to the active subcarriers in the g^{th} sub-block, respectively. The g^{th} OFDM-IM sub-block generates the frequency domain data, which are then concatenated from $g = 1$ to $g = G$, before putting into the IFFT block. Normal Cyclic Prefix (CP) insertion and parallel to serial conversion are then followed in order to synthesize the desired OFDM-IM signal waveforms in the time domain.

In the communication processor module of the far-field Rx, the 'Index Demod' comprises two parts: received signals separation and index detector. The received signals are separated according to different frequencies of each OFDM-IM sub-block Creator, before the active subcarrier indices from each sub-block are detected independently in the index detector. Here an additive white Gaussian noise (AWGN) channel is considered. While in the Radar processor, a signal processing module which connects two access points gaining the transmitted/received data is equipped to obtain Radar range-velocity profile.

It should be noted that in the proposed OFDM-IM RadCom, when $G = 1$, the bit stream D is modulated directly without dividing into multiple groups. In this case, p_1 bits are mapped upon the active subcarrier indices out of the total number of OFDM subcarrier indices. Compared with this special case, OFDM-IM RadCom with $G > 1$ can obtain more evenly distributed active subcarrier indices across the entire subcarrier range, thereby maintaining reasonable Radar performance. Therefore, in this paper, we choose to demonstrate the Radar performance of the proposed RadCom with $G > 1$. We assume $N = 64$, while the number of sub-blocks G is chosen to be 32, 16, 8, and 4. Other parameters are listed in Table 2.

In the following analysis, the performance of the proposed OFDM-IM RadCom is studied. Specifically, Section 3 is devoted to the Radar performance and the PA efficiency.

3 Radar performance and PA efficiency

In this section, the OFDM-IM RadCom waveform performance is firstly evaluated by way of computing its ambiguity function [17]. Then we focus on using CS method to obtain the Radar range-velocity profile in the proposed OFDM-IM RadCom system. Moreover, PA efficiency is also studied.

3.1. Radar performance

The Radar waveform performance is commonly obtained from the ambiguity function. Ambiguity function is defined as the envelope of the matched filter output when the input to the filter is a time-delayed and Doppler-shifted version of the original signal, to which the filter was matched [18]. It can be mathematically expressed as

$$\chi(\tau, \upsilon) = \left| \int_{-\infty}^{\infty} x(t) x^*(t+\tau) \exp(j2\pi\upsilon t)\, dt \right|, \tag{7}$$

where τ is the propagation time delay between the reflected signal from the distant target and the original transmitted signal $x(t)$. v denotes the Doppler frequency shifts due to the relative velocity between the transmitter and the target. Positive v here indicates an approaching target, and vice visa. '*' refers to the complex conjugate operator.

The ambiguity function definition in (7) is applicable to both the classical OFDM and the proposed OFDM-IM systems. The only difference is that the time-domain signals $x(t)$, are the summation of all, for the OFDM, or a subset of, for the OFDM-IM, modulated orthogonal subcarriers. The $x(t)$ for the OFDM and the OFDM-IM are, respectively, expressed as in (1) and (8)

$$x(t) = \sum_{\mu=0}^{N_{\text{sym}}-1} \sum_{\beta} a_{(\mu,\beta)} \exp(j2\pi f_{\beta} t)\,\text{rect}\left(\frac{t-\mu T}{T}\right). \tag{8}$$

Here, β is the active subcarrier index, $\beta \in \{0, 1, \ldots, N-1\}$. Since the active subcarrier indices are dynamically updated according to the incoming bits, K different values of β from 0 to $N-1$ can be selected for each symbol.

Using the ambiguity function, we can compare the Radar performance of the proposed OFDM-IM RadCom waveform to the classical OFDM RadCom waveform. In order to ensure subcarrier orthogonality, the frequency spacing Δf between the adjacent subcarriers needs to be at least 10 times greater than f_{D} [19]. Here f_{D} denotes the maximum Doppler shift. As an illustrative example, we assume the required detectable range R is 105 m, which requires a CP length T_{cp} of greater than $2R/c_0 = 0.7$ us [20], where c_0 is the speed of light.

Table 3 Example OFDM-IM and OFDM RadCom system parameters.

Parameters	Symbols	Value
Carrier frequency	f_0	24 GHz
Number of subcarriers	N	64
Number of evaluated symbols	N_{sym}	256
Minimum subcarrier spacing	Δf	312.5 kHz
Data symbol duration	T_{d}	3.2 μs
Cyclic prefix length	T_{cp}	0.8 μs
Total Symbol duration	T	4 μs
Total signal bandwidth	B	≤ 20 MHz

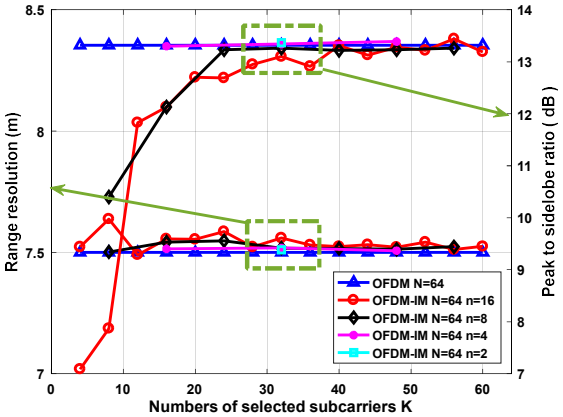

Fig. 3 *Ambiguity function, range resolutions/PSLs of OFDM and OFDM-IM RadComs for various n and k. N is fixed as 64.*

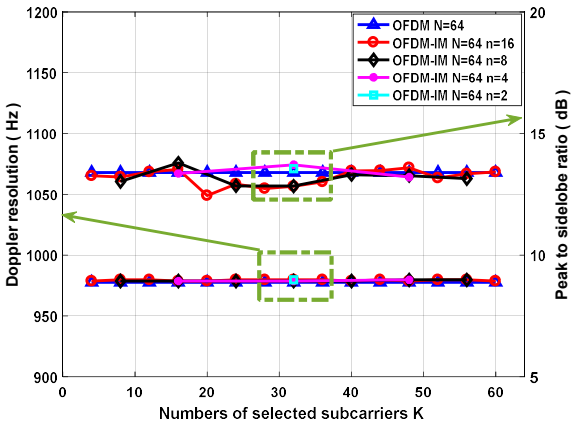

Fig. 4 *Ambiguity function, Doppler resolutions/PSLs of OFDM and OFDM-IM RadComs for various n and k. N is fixed as 64.*

The performance of the proposed OFDM-IM RadCom, using metrics of range/Doppler resolution and PSL, is compared with those obtained with the classical OFDM RadCom in Figs. 3 and 4 for various n (or G, as $G = N/n$) and k. The other system parameters used in simulations are listed in Table 3. It should be noted that the signal frequency bandwidth B of the classical OFDM RadCom is 20 MHz, while the proposed OFDM-IM RadCom has B no larger than 20 MHz, because the actual frequency bandwidth B is determined by the active subcarriers that are dynamically updated. For example, when the subcarrier at the edge of the band is deactivated, the actual bandwidth is less than 20 MHz. Thus, only maximum occupied bandwidth can be given in the OFDM-IM RadCom system.

As seen from Figs. 3 and 4, the proposed OFDM-IM RadCom examples have similar level of resolution and PSL in both the range and Doppler domains as the classical OFDM RadCom system. For range domain PSLs, OFDM-IM RadCom also requires small n and large k. This is because the greater the number of sub-blocks G (smaller n) and selected subcarriers, the more evenly the active subcarriers are distributed across the operational frequency bandwidth, resulting in similar occupied frequency bandwidth. The bandwidth is the determining factor to the system Radar performance.

While, in the conventional OFDM RadCom system, the modulation symbol-based processing approach is employed to estimate the range-velocity profile, which enjoys a high gain in Radar signal processing [1]. In this approach, the $N \times N_{\text{sym}}$ matrix D_{div} carrying the range and velocity information can be obtained through an element-wise complex division. Wherein, D_{div} can be expressed as [1, (20)] (attenuation is normalised out),

$$\left(D_{\text{div}}\right)_{\eta+1,\mu+1} = \vec{D}_{\text{R}} \otimes \vec{D}_{\text{D}} \quad \eta = 0,1,2,\cdots N-1, \quad \mu = 0,1,2,\cdots N_{\text{sym}}-1 \tag{9}$$

where

$$D_{\text{R}}(\eta+1) = \exp(-j2\pi\eta\Delta f \frac{2R}{c_0}) \tag{10}$$

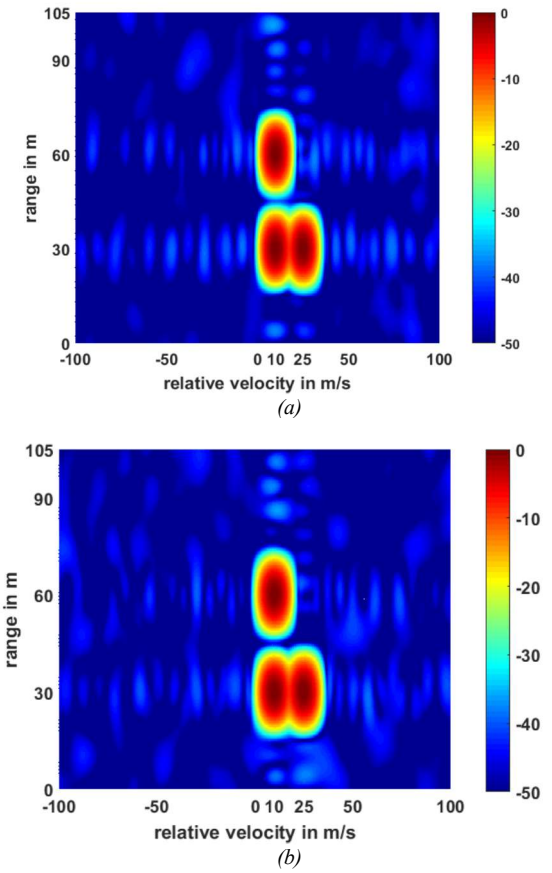

Fig. 5 *Normalised Radar range-velocity image for 3 targets (SNR = 10 dB) with R = (30 m, 30 m, 60 m) and v_{rel} = (10 m/s, 25 m/s, 10 m/s), level in dB. (a) OFDM-IM with compressed sensing approach. (b) OFDM with modulation symbol based processing approach.*

and

$$D_{\mathrm{D}}(\mu+1) = \exp(j2\pi\mu T \frac{2v_{\mathrm{rel}} f_{\mathrm{c}}}{c_0}). \tag{11}$$

'⊗' refers to a dyadic product. The joint range-velocity information of targets can be gained via the straightforward discrete Fourier transform (DFT) and inverse discrete Fourier transform (IDFT). However, in the proposed OFDM-IM RadCom system, the inactive subcarriers produce zero entries in the matrix D_{div}. In each column of D_{div}, the subcarrier indices are randomly selected, thus the frequency spacing of each two consecutive active subcarriers could be different when discarding the zero elements prior to IDFT operation. This characteristic would result in an exacerbation of PSL level in the range domain after the IDFT is applied. In each row of D_{div}, similarly, only poor velocity profile can be obtained when removing the zero elements and compute DFT as the order of the OFDM symbol indices is distorted in every row of D_{div}. To obtain the full OFDM range-velocity profile performance from the OFDM-IM signal compressed sensing (CS) method is used. As is known, in order to applying CS method, the signal must be sparse in some transformation domains [21]. While, in the proposed OFDM-IM RadCom system, besides the random property of the frequency, the Radar signals are sparse in the joint range-velocity domain since the range-velocity measurement space consists only a

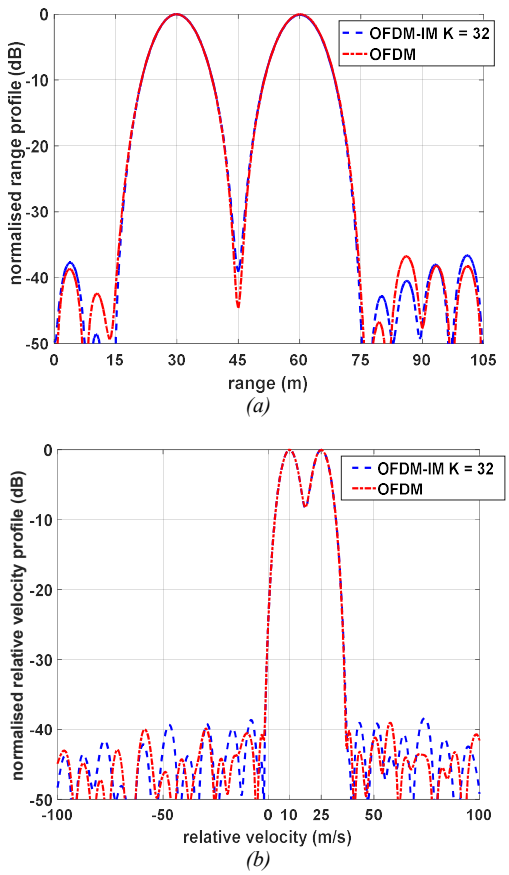

Fig. 6 *(a) Constant relative velocity cut at v_{rel} = 10 m/s and (b) constant range cut at R = 30 m of the OFDM-IM and the OFDM Radar images.*

few of potential targets, e.g. in automotive applications [22], [23]. In the OFDM-IM RadCom, the zero entries in the matrix D_{div} due to the inactive subcarriers are discarded then we get the $K \times N_{\mathrm{sym}}$ matrix B_{cs} which can be expressed as

$$B_{\mathrm{cs}} = [b_1\ b_2\ \ldots\ b_{\mu+1}\ \ldots\ b_{\mathrm{Nsym}}], \tag{12}$$

where $b_{\mu+1} \in \mathbb{C}^{K\times 1}$. In order to obtain the full OFDM Radar performance, the basis pursuit problem (BPP) here is

$$\min_{r_{\mu+1}\in\mathbb{C}^N} \left\| r_{\mu+1} \right\|_1, \text{ s.t. } A \cdot r_{\mu+1} = b_{\mu+1}. \tag{13}$$

In (13), $r_{\mu+1} \in \mathbb{C}^{N\times 1}$ is the wanted spatial spectrum vector. $A \in \mathbb{C}^{K\times N}$ is a submatrix of the DFT matrix $W_{\mathrm{N}} \in \mathbb{C}^{N\times N}$ and $A = W_{\mathrm{N}}(\beta + 1, \eta + 1)$. $\|\cdot\|_1$ denotes the ℓ_1-norm. In order to solve the BPP, the YALL1 algorithm is employed [24], [25]. Through applying CS, we get the matrix $D_{\mathrm{cs}} = [r_1\ r_2\ \ldots\ r_{\mu+1}\ \ldots\ r_{\mathrm{Nsym}}]$ in the frequency domain. When we transform the data into the time domain denoted as matrix D_{Tcs}, the Radar range-velocity profile can be obtained via IDFT (of each column of D_{Tcs}) followed by a DFT processing (of each row of D_{Tcs}).

In order to validate the effectiveness of the CS method, the range-velocity profile obtained from the proposed OFDM-IM RadCom with CS processing is simulated in Fig. 5*(a)*. For comparison purpose, the OFDM RadCom Radar image calculated with modulation symbol based processing is described in Fig. 5*(b)*. It is assumed that three targets respectively locate at range of R = (30 m, 30 m, 60 m) with

relative velocity of v_{rel} = (10 m/s, 25 m/s, 10 m/s) and SNR = 10 dB. In this example, the OFDM-IM RadCom system is designed with $N = 64$, $K = 32$. In Fig. 6, the constant relative velocity and range cuts of the OFDM-IM and the OFDM Radar images shown in Fig. 5 are depicted. Compared with the conventional OFDM RadCom, it can be observed that similar PSL levels and range resolutions are obtained in the OFDM-IM RadCom when CS method is adopted. Meanwhile, the proposed OFDM-IM RadCom also achieves similar velocity profile to that in the OFDM RadCom which can be observed in Fig. 6*(b)*. Hence, the proposed OFDM-IM RadCom with CS method can achieve similar performance to the OFDM RadCom on Radar processing aspect. On the other hand, the OFDM-IM processing may require extra computational resources to perform the YALL1 algorithm in addition to the two-dimensional (2-D) fast Fourier transform (FFT) operation. When comparing the OFDM-IM with the multiple-input multiple-output (MIMO) scheme, i.e. regularly spaced active subcarriers proposed in [26], since the maximum unambiguous measurement range in the MIMO scheme is reduced due to the adverse impact of the factor N_{ch} defined as the number of orthogonal transmit channels, the OFDM-IM can achieve greater maximum detectable range.

3.2. PA efficiency

It is well known that OFDM signals are high peak-to-average-ratio (PAPR) waveforms. As a consequence, in order to retain acceptable RF chain linearity, the PAs have to operate at high back-off points, resulting in poor PA energy efficiencies. In conventional OFDM systems, the maximum PAPR occurs when all of the N subcarriers are phase aligned, resulting in PAPR = N (assuming each subcarrier has identical power). In the OFDM-IM system, because less subcarriers, i.e. less than N, are activated during transmission, the associated maximum PAPR can be reduced accordingly. The PAPR of a signal waveform can be expressed as

$$PAPR = \frac{\max\left|x(t)e^{j2\pi f_0 t}\right|^2}{E\left[\left|x(t)e^{j2\pi f_0 t}\right|^2\right]}, \tag{14}$$

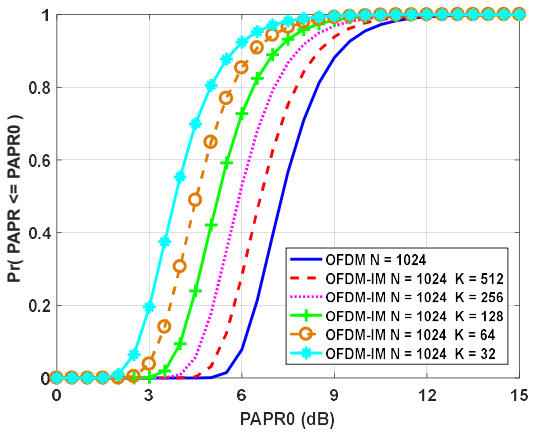

Fig. 7 *CDF of the PAPR of the proposed OFDM-IM and OFDM systems.*

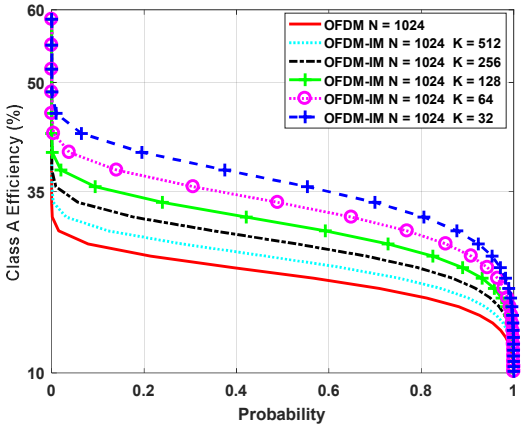

Fig. 8 CDF of *Class-A PA efficiency for the example OFDM-IM and OFDM signals shown in Fig. 7.*

where '$E[\cdot]$' takes expectations over a sufficient long time period. f_0 refers to the RF carrier frequency. An approximate expression was derived for the cumulative distribution function (CDF) of PAPR of OFDM signals in [6], [12]. In consonance with the central limit theorem, assuming that the real and imaginary parts of $x(t)e^{j2\pi f_0}$ respectively follow Gaussian distributions, each with a mean of zero and variance of 0.5 for a large number of subcarriers. Thus, the magnitude of $x(t)e^{j2\pi f_0}$ has a Rayleigh distribution and the power distribution enjoys a central chi-square distribution with two degrees of freedom. Therefore, the CDF of the magnitude of a signal sample can be expressed as

$$F(\text{PAPR}0) = 1 - e^{-\text{PAPR}_0}, \tag{15}$$

where PAPR_0 is a predefined threshold value. It is assumed that K signal samples in time domain are mutually independent and uncorrelated. Then the CDF of the PAPR of a data block can be given by

$$Prob\ (\text{PAPR} \leqslant \text{PAPR}0) = (1 - e^{-\text{PAPR}_0})^K. \tag{16}$$

In Fig. 7, we present the theoretical CDFs of PAPR of the proposed OFDM-IM system with different number of selected subcarriers. It is shown that the proposed OFDM-IM waveform offers a lower average PAPR than the classical OFDM waveform.

Therefore, compared to classical OFDM RadCom, the proposed OFDM-IM RadCom system here with its lower PAPR should enjoy a higher PA efficiency [27], [28]. The theoretical relation between the PA efficiency and the PAPR is plotted in [27, Fig. 1]. As an example, the class-A PA efficiency α can be described as

$$\alpha = Q\exp(-q \cdot \chi_{\text{dB}}), \tag{17}$$

with χ_{dB} denoting the PAPR in dB. For the class-A operation, Q = 58.7% and q = 0.1247 [28]. Fig. 8 presents the CDF of PA efficiency simulation for the signals in Fig. 7. As seen from Fig. 8, the proposed OFDM-IM RadCom transmitter has a higher PA efficiency than that achieved for a classical OFDM RadCom transmitter.

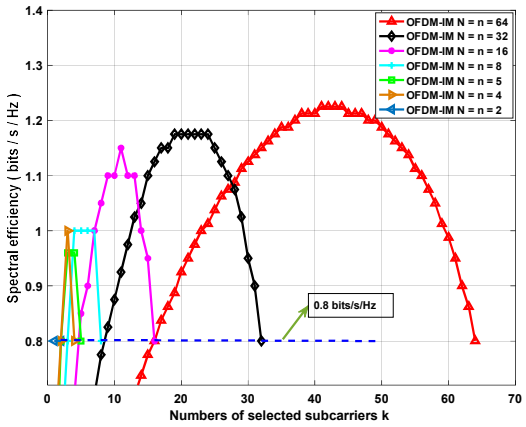

Fig. 9 *Spectral efficiency of the proposed OFDM-IM RadCom for various settings.*

4 Spectral efficiency and BER

In this section, the spectral efficiency and bit error rate (BER) are simulated to evaluate the communication performance of the proposed OFDM-IM RadCom system under BPSK modulation.

4.1. Spectral efficiency

In the proposed OFDM-IM RadCom, the selected subcarriers are used for conveying binary data, with spectral efficiency of $D/(N + L_{cp})$ [8]. L_{cp} is the length of CP which is appended after the IFFT operation. The OFDM is a special case of OFDM-IM, i.e. $K = N$. For the classic OFDM system, assuming $N = 64$, $L_{cp} = 16$, the OFDM system can achieve a spectral efficiency value $64/(64 + 16) = 0.8$ bits/s/Hz for BPSK modulation. In one symbol duration, compared with the conventional OFDM, for example, when $N = n = 64$ and $k = 40$, the selected k subcarriers can convey $(40 + 57)$ data bits, i.e., $D = 97$ bits, wherein the 40 bits and 57 bits respectively represent the mapped bits and modulated bits by the signal constellations and the active subcarrier indices. Hence, in this OFDM-IM case, the spectral efficiency value, i.e., 1.21 bits/s/Hz can be achieved, higher than that in the OFDM system, i.e. 0.8 bits/s/Hz. Seen from Fig. 9, spectral efficiency of the OFDM-IM system is quadratic in form with increasing number of selected subcarriers k. When the proper number of subcarriers are selected, the system can achieve higher spectral efficiency than can be achieved by the OFDM system.

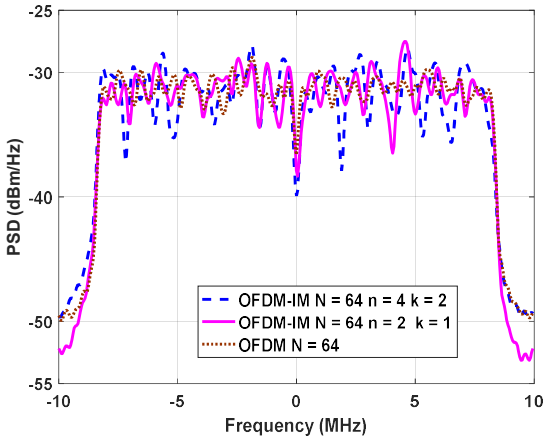

Fig. 10 *PSD of OFDM (IEEE 802. 11a) and OFDM-IM (five symbols).*

4.2. BER

In [29], an averaged simulation result showing that the performance of spectral containment of the conventional OFDM and the OFDM-IM are similar. In order to see the characteristic of in-band power spectral density (PSD), here the PSD levels of the conventional OFDM and the OFDM-IM for five symbols are depicted which is shown in Fig. 10. It can be observed that when the same transmit power is allocated to the OFDM symbol, the out-of-band emission (OOBE) leakage of the OFDM has similar performance to that of the OFDM-IM, which was also proved in [30]. The OFDM-IM may have larger in-band ripple than that in the OFDM because of the dynamically activated subcarriers in the OFDM-IM and the power allocation strategy used. In this paper, a given identical transmit power budget is assumed for each transmitted bit and only AWGN is considered for the presented BER performance in the RadCom system. In the proposed OFDM-IM RadCom system, the transmit power needs to be re-allocated since some parts of the transmitted bits are conveyed by the subcarrier indices. In order to have a fair comparison with other systems, we adopt an identical equivalent system bit energy E_{IMb} across different systems [12]. The relationship between E_{IMb} and E_b (which is the bit energy without considering power redistribution) is given by

$$E_{IMb} = \frac{(p_1 + p_2)}{p_2} E_b = \frac{p}{p_2} E_b . \tag{18}$$

Within the Rx communication processor, decision errors could occur on both active subcarrier indices detection and on constellation symbols recovery. The BER P_b associated with each sub-block can be expressed as

$$P_b = \frac{P_e}{P} , \tag{19}$$

where P_e denotes the total number of bit errors which comprises two parts, say P_{1e} and P_{2e}. P_{1e} denotes the total number of bit errors caused by the incorrectly recovered subcarrier indices, and P_{2e} denotes the number of erroneous bits detected for M-ary symbols. P is the total transmitted bits in each sub-block.

In the 'Index Demod' module in Fig. 2, square-law envelope detectors are employed in each received sub-block to identify the active subcarriers. The subcarrier indices associated with the k largest power in the frequency domain are recovered as the subcarrier indices that are activated at the transmitter side [12]. As we have discussed the number of unused index combinations, i.e. $C(n, k) - c$, could cause numerical overflow which considerably increase P_{1e} if untreated. Therefore, in the following, an algorithm to eliminate numerical overflow of active index combinations is described.

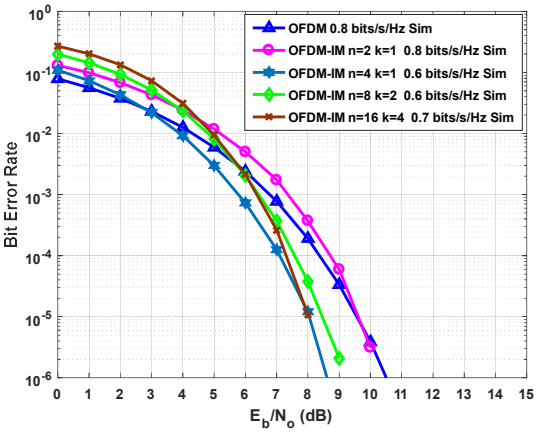

Fig. 11 *BER performance of OFDM-IM and OFDM RadComs for various configurations.*

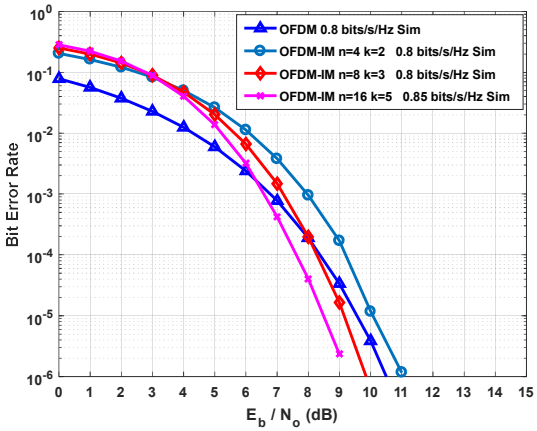

Fig. 12 *BER performance of OFDM-IM and OFDM RadComs for various configurations.*

Assume the subcarrier frequency power received in the frequency domain is a set V of $\{v_n, v_{n-1}, \ldots, v_1\}$, where $v_n > v_{n-1} > \ldots > v_1$. The corresponding subcarrier index sequence is $J_n = \{j_n, j_{n-1}, \ldots, j_1\}$. And J_k is the recovered active subcarrier index sequence in the communication processor which contains k elements, i.e., $j_n, j_{n-1}, \ldots, j_{n-k+1}$.

1) Detect if the overflow occurs: A decimal number c' of J_k is calculated by using $c' = C(j_n, k) + C(j_{n-1}, k-1) + \ldots + C(j_{n-k+1}, 1)$. If $c' > 2^{p_1} - 1$, the overflow occurs, and go to 2). Otherwise, J_k is determined as the recovered subcarrier index sequence;
2) Find out the subcarrier indices which cause the numerical overflow. Comparing the combination number of each element in J_k, $C(j_n, k)$, … , $C(j_{n-k+1}, 1)$, with the overflow value Δc, defined as $\Delta c = c' - (2^{p_1} - 1)$. Pick out the elements whose combination number greater than Δc and preserving them into a vector J_l. J_l denotes the possible erroneous index sequence which contains l elements, with V_l representing the power of the corresponding subcarriers;
3) The smallest value element in V_l which is associated with the index $j_a, j_a \in J_k$, is determined as the first index element to be replaced with the $(k + \varepsilon)^{th}$ element of J_n. That is because among all the values in V_l, a greater value means it is more likely that the corresponding index is correct. Thus a new sequence of J_k is obtained. Then go to 1) with $\varepsilon = \varepsilon + 1$. ε is initialized as 1, and the iteration terminates when ε reaches $n - k$.

In Figs. 11 and 12, we compare the BER performance of the proposed OFDM-IM RadCom with the OFDM approach when BPSK modulated for different spectral efficiency values. As seen from Fig. 11, for the spectral efficiency values of 0.6 bits/s/Hz and 0.7 bits/s/Hz, the OFDM-IM RadCom example can provide significant BER improvement. Seen from Fig. 12, for a higher spectral efficiency of 0.85 bits/s/Hz, OFDM-IM RadCom with $n = 16$, $k = 5$ can achieve around 1 dB SNR gain compared with OFDM at BER of 10^{-5}. Meanwhile, we observe from Figs. 11 and 12, at a BER value of 10^{-6} OFDM-IM RadCom with $n = 2$, $k = 1$ and $n = 8$, $k = 3$ obtains better BER performance than OFDM operating at the same spectral efficiency. This is due to the contribution of the total equivalent system bit energy. For OFDM-IM RadCom with $n = 2$, $k = 1$, the equivalent system bit energy is doubled when compared with classical OFDM, while for $n = 8$, $k = 3$, it is 4.3 dB higher. Moreover, even though the $n = 2$, $k = 1$ and $n = 4$, $k = 2$ have the same equivalent system bit energy, the BER performance is still different. That happens because the percentages of the number of unused combinations out of the all possible index combinations are different, i.e. 33.3% for $n = 4$, $k = 2$ and 0 for $n = 2$, $k = 1$. Therefore, OFDM-IM with $n = 2$, $k = 1$ can achieve better BER performance. Additionally, seen from Figs. 11 and 12, in the low SNR region of 0 to 5 dB, the OFDM-IM RadCom has a compromised BER performance. This can be explained by the fact that for low SNR, the BER performance of the OFDM-IM RadCom system is dominated by the bit errors caused by incorrectly recovered subcarrier indices. On the other hand, the OFDM-IM RadCom system achieves better BER performance than the OFDM RaCom system when the SNR is greater than 5 dB. This is because the improved error performance of the bits transmitted in the index domain, indicating that conveying information bits by the indices of the subcarriers is more effective at high SNR.

5 Conclusion

A new system named OFDM-IM RadCom that integrates Radar sensing and wireless communication is investigated in this paper. Here since fewer OFDM subcarriers are activated higher spectral efficiency and better BER performance could be obtained when system parameters are properly selected. It was also shown that the proposed system achieves approximately the same performance in Radar range and velocity profiles in comparison to standard OFDM RadCom. OFDM-IM thus appears to offer an efficient method for next generation combinatorial Radar-communications systems that may be required for applications such as autonomous vehicle control.

6 Acknowledgments

Mr. G. Huang's work was supported by the National Natural Science Foundation of China under Grant no.61871425, the Guangxi BaGui Scholars Foundation, the Study Abroad Program for Graduate Student from Guilin University of Electronic Technology (GUET), China, and the

Innovation Project of GUET Graduate Education. Dr. Y. Ding's work was supported by Heriot-Watt University Academic Start-up funding, and the EPSRC (UK) under Grant EP/P025129/1.

7 References

[1] Sturm, C., Wiesbeck, W.: 'Waveform design and signal processing aspects for fusion of wireless communications and Radar imaging', *Proc. IEEE*., 2011, **99**, (7), pp. 1236–1259

[2] Han, L., Wu, K.: 'Joint wireless communication and Radar sensing systems-state of the art and future prospects', *IET Microw. Antennas Propag*., 2013, **7**, (11), pp. 876–885

[3] Saddik, G.N., Singh, R.S., Brown, E.R.: 'Ultra-wideband multifunctional communications/radar system', *IEEE Trans. Microw. Theory Tech*. MTT, 2007, **55**, (7), pp. 1431–1437

[4] ''Self-driving' lorries to be tested on UK roads'. Available at https://www.bbc.co.uk/news/technology-41038220, accessed 25 August 2017

[5] Sturm, C., Zwick, T., Wiesbeck, W.: 'An OFDM system concept for joint radar and communications operations'. Proc. IEEE 69th Veh. Technol. Conf., Barcelona, Spain, April 26–29, 2009, pp.1–5

[6] Han, S.H., Lee, J.H.: 'An overview of peak-to-average power ratio reduction techniques for multicarrier transmission', *IEEE Wireless Commun*. 2005, **12**, (2), pp. 56–65

[7] Jiang, T., Wu, Y.: 'An overview: Peak-to-Average power ratio reduction techniques for OFDM signals', *IEEE Trans. Broadcast.*, 2008, **54**, (2), pp. 257–268

[8] Başar, E., Aygölü, Ü., Panayırcı, E., *et al*.: 'Orthogonal frequency division multiplexing with index modulation', *IEEE Trans. Signal Process*., 2013, **61**, (22), pp. 5536–5549

[9] Domouchtsidis, S.G., Ntouni, G.D., Kapinas, V.M., *et al*.: 'OFDM-IM vs FQAM: A comparative analysis'. Proc. 23rd Int. Conf. Telecoms., Thessaloniki, Greece, May 16–18, 2016, pp. 1–5

[10] Basar, E.: 'On multiple-input multiple-output OFDM with index modulation for next generation wireless networks', *IEEE Trans. Signal Process*., 2016, **64**, (15), pp. 3868–3878

[11] Wen, M., Cheng, X., Ma, M., *et al*.: 'On the achievable rate of OFDM with index modulation', *IEEE Trans. Signal Process*., 2016, **64**, (8), pp. 1919–1932

[12] Soujeri, E., Kaddoum, G., Au, M., *et al*.: 'Frequency index modulation for low complexity low energy communication networks', *IEEE Access.*, 2017, vol. 5, pp. 23276–23287

[13] Rappaport, T.S., Annamalai, A., Buehrer, R.M., *et al*.: 'Wireless communications: past events and a future perspective', *IEEE Commun. Mag.*, 2002, **40**, (5), pp. 148–161

[14] Levanon, N.: 'Multifrequency complementary phase-coded radar signal', *IEE Proc., Radar Sonar Navig*., 2000, **147**, (6), pp. 276–284

[15] Lellouch, G., Tran, P., Pribic, R., *et al*.: 'OFDM waveforms for frequency agility and opportunities for Doppler processing in radar'. Proc. IEEE Radar Conf., Rome, May 26–30, 2008, pp. 1–6

[16] Sit, Y. L., Nuss, B., Zwick, T.: 'On mutual interference cancellation in a MIMO OFDM multiuser radar-communication network', *IEEE Trans. Veh. Technol.*, 2018, 67, (4), pp. 3339–3348

[17] Johnson, N., Chergui, M., Sternberg, O., *et al*.: 'Ambiguity function analysis for passive radar system performance.' Proc. 2016 IEEE Military Communications Conf., 2016, pp. 872–876

[18] Sinsky, A.I., Wang, C.P.: 'Standardization of the Definition of the Radar Ambiguity Function', *IEEE Trans. Aerosp. Electron. Syst*., 1974, vol. AES–10, no. 4, pp. 532–533

[19] Braun, M., Sturm, C., Niethammer, A., *et al*.: 'Parametrization of joint OFDM-based radar and communication systems for vehicular applications'. Proc. IEEE 20th Int. Symp. on Personal Indoor Mobile Radio Commun., Tokyo, Japan, Sep. 13–16, 2009, pp. 3020–3024

[20] Tigrek, R.F., de Heij, W.J.A., van Genderen, P.: 'Solving Doppler ambiguity by Doppler sensitive pulse compression using multi-carrier waveform'. Proc. Eur. Radar Conf., Amsterdam, Netherlands, October 30–31, 2008, pp. 72–75

[21] Donoho, D.L.: 'Compressed sensing', *IEEE Trans. Inf. Theory*, 2006, **52**, (4), pp. 1289–1306

[22] Knill, C., Schweizer, B., Sparrer, S., et al.: 'High range and Doppler resolution by application of compressed sensing using low baseband bandwidth OFDM radar', *IEEE Trans. Microw. Theory Tech.*, 2018, **66**, (7), pp. 3535–3546

[23] Nuss, B., Sit, L., Zwick, T.: 'A novel technique for interference mitigation in OFDM radar using compressed sensing'. Proc. 2017 IEEE MTT-S Int. Conf. Microw. Intell. Mobility (ICMIM)., March 2017, pp. 143–146

[24] Yang, J., Zhang, Y.: 'Alternating direction algorithms for L1-problems in compressive sensing', *SIAM J. Sci. Comput.*, 2011, **33**, (1), pp. 250–278

[25] 'Your ALgorithms for L1'. Available at: http://yall1.blogs.rice.edu, accessed 1 December 2020

[26] Sturm, C., Sit, Y. L., Braun, M., et al.: 'Spectrally interleaved multi-carrier signals for radar network applications and multi-input multi-output radar', *IET Radar Sonar Navig.*, 2013, **7**, (3), pp. 261–269

[27] Miller, S. L., O'Dea, R.J.: 'Peak Power and Bandwidth Efficient Linear Modulation', *IEEE Trans. Commun*., 1998, **46**, (12), pp. 1639–1648

[28] Wulich, D.: 'Definition of efficient PAPR in OFDM', *IEEE Commun. Lett*., 2005, **9**, (9), pp. 832–834

[29] Gokceli, S., Basar, E., Wen, M., *et al*.: 'Practical implementation of index modulation-based waveforms', *IEEE Access*., 2017, vol. 5, pp. 25463–25473

[30] Jaradat, A.M., Hamamreh, J.M., Arslan, H.: 'Modulation options for OFDM-based waveforms: classification, comparison, and future directions', *IEEE Access*, 2019, vol. 7, pp. 17263–17278